

Relaxation in Ordered Assembly of Magnetic Nanoparticles

Manish Anand*

*Department of Physics, Bihar National College,
Patna University, Patna-800004, India.*

(Dated: June 29, 2021)

Abstract

We study the relaxation characteristics in the two-dimensional ($l_x \times l_y$) array of magnetic nanoparticles (MNPs) as a function of aspect ratio $A_r = l_y/l_x$, dipolar interaction strength h_d and anisotropy axis orientation using computer simulation. The anisotropy axes of all the MNPs are assumed to have the same direction, α being the orientational angle. Irrespective of α and A_r , the functional form of the magnetization-decay curve is perfectly exponentially decaying with $h_d \leq 0.2$. There exists a transition in relaxation behaviour at $h_d \approx 0.4$; magnetization relaxes slowly for $\alpha \leq 45^\circ$; it relaxes rapidly with $\alpha > 45^\circ$. Interestingly, it decays rapidly for $h_d > 0.6$, irrespective of α . It is because the dipolar interaction promotes antiferromagnetic coupling in such cases. There is a strong effect of α on the magnetic relaxation in the highly anisotropic system ($A_r \geq 25$). Interesting physics unfolds in the case of a huge aspect ratio $A_r = 400$. There is a rapid decay of magnetization with α , even for weakly interacting MNPs. Remarkably, magnetization does not relax even with a moderate value of $h_d = 0.4$ and $\alpha = 0^\circ$ because of ferromagnetic coupling dominance. Surprisingly, there is a complete magnetization reversal from saturation (+1) to -1 state with $\alpha > 60^\circ$. The dipolar field and anisotropy axis tend to get aligned antiparallel to each other in such a case. The effective Néel relaxation time τ_N depends weakly on α for small h_d and $A_r \leq 25.0$. For large A_r , there is a rapid fall in τ_N as α is incremented from 0 to 90° . These results benefit applications in data and energy storages where such controlled magnetization alignment and desired structural anisotropy are desirable.

*Electronic address: itsanand121@gmail.com

I. INTRODUCTION

In recent years, there has been much research interest in two-dimensional arrays of magnetic nanoparticles (MNPs) due to their diverse technological applications such as spintronics, magnetic hyperthermia, drug delivery, data storage, etc. [1–7]. In these contexts, relaxation characteristics of the underlying system are one of the essential quantifiers [8, 9]. The latter is primarily characterized by a time scale known as Néel relaxation time, which depends strongly on various parameters of interest such as particle size, thermal fluctuations, anisotropy strength, magnetic interaction, etc. [10–12]. Therefore, the investigation of magnetic relaxation in such a system represents a topic of practical importance.

The magnetic relaxation properties are well understood in the case of non-interacting MNPs [13, 14]. However, MNPs are found to interact primarily via dipole-dipole interaction in an assembly. The dipolar interaction has varied effects on various thermodynamical and magnetic properties of crucial importance because of its long-range and anisotropic behaviour [15, 16]. For instance, it imparts spin-glass like character in randomly distributed MNPs [17, 18]. On the other hand, it plays a crucial role in determining the morphology of magnetic ordering [19, 20]. Holden *et al.* studied the ground state spin structures in two-dimensional kagome lattice using Monte Carlo simulation. They observed six-fold degenerate spin states because of dipolar interaction [21]. Bailly-Reyre *et al.* found ground-state configuration to be a vortex in the cubic assembly of nanodots [22]. Luttinger *et al.* observed the minimum energy configurations to be ferromagnetic in a face-centred cubic lattice [23]. In contrast, it is antiferromagnetic in a simple cubic arrangement of MNPs [23]. It promotes antiferromagnetic spin states in a square array, while for a triangular arrangement, the minimum energy configuration is ferromagnetic [24, 25]. The dipolar interaction may induce ferromagnetic or antiferromagnetic coupling among the MNPs depending on their relative positions. Consequently, the magnetic relaxation properties of interacting MNPs not only depends on interaction strength but also on the spatial configuration of particles [26].

Various research works suggest that the dipolar interaction affects the relaxation characteristics in an assembly of MNPs strongly [27–29]. For example, Gallina *et al.* theoretically investigated the magnetization dynamics and interaction energy landscapes in a two-dimensional assembly of dipolar interacting MNPs [30]. Magnetic relaxation is found to follow stretched exponential law in weakly disordered systems. Using computer simula-

tions, Patrick Ilg studied the relaxation dynamics of multicore magnetic nanoparticles [31]. The magnetic relaxation is well characterized by an exponentially decaying function for moderate dipolar interaction strength. Denisov *et al.* probed the relaxation properties in two-dimensional assembly using mean-field approximations [32]. They observed a two-distinct relaxation time scale. Shtrikmann *et al.* and Dormann *et al.* investigated the magnetic relaxation in an interacting assembly using theoretical calculations [33, 34]. They also observed an elevation in relaxation time due to dipolar interaction. On the other hand, Mørup *et al.* observed a decrease in relaxation time with an increase in dipolar interaction strength [35]. In recent work, we studied magnetic relaxation in the two-dimensional assembly of MNPs as a function of dipolar interaction strength and aspect ratio of the system with randomly oriented anisotropy axes [36]. The dipolar interaction of enough strength increases or decreases the relaxation time depending on the aspect ratio of the system.

Some recent works also indicate that the orientation of anisotropy axes plays a crucial role in determining various magnetic properties of interest [37–39]. It is also strengthened from the fact that the magnetic field promotes some degree of orientation of elongated structures along the field direction [40–42]. Conde-Leborán *et al.* studied the heating efficiency in the assembly of interacting MNPs as a function of the degree of collinearity of their easy axes [42]. The amount of heat dissipation depends strongly on the anisotropy axes orientation for weakly interacting MNPs. Boekelheide *et al.* investigated the effect of anisotropy axes orientation on the hysteresis loops using micromagnetic simulations and experiments [43]. The coercivity is found to significantly modified by the direction of anisotropy axes. Using experiments, Li *et al.* studied the hysteresis response in dense arrays of magnetic nanowires [44]. The coercive field and remanent magnetization are more significant with perfectly aligned anisotropy as compared to perpendicular orientation. Allia *et al.* analyzed the hysteresis properties in an assembly of MNPs with aligned and randomly oriented anisotropy axes [45]. The hysteresis loop area is enormous with aligned anisotropy axes as compared to the random orientation case. Using kinetic Monte Carlo simulations and analytical calculations, we studied the magnetic relaxation in the linear chain of nanoparticles as a function of anisotropy axis orientation and dipolar interaction strength [46]. There is a fastening or slowing down of magnetization relaxation depending on the angle between the anisotropy axis and the particles array.

It is evident from above discussions that the dipolar interaction and anisotropy axes

orientation strongly affect the magnetic relaxation characteristics in ordered arrays of MNPs. However, a complete understanding of the effect of these factors is still lacking. Thus motivated, we systematically analyzed the effect of dipolar interaction, the orientation of anisotropy axes, and the aspect ratio of the system on the relaxation mechanism in two-dimensional assembly of MNPs using kinetic Monte Carlo (kMC) simulation in the present work. We also investigate the variation of effective Néel relaxation time τ_N as a function of these parameters.

The rest of the paper is organized as follows: We discuss the model and various energy terms in Sec. II. The simulation method is also discussed in brief. The numerical results are analyzed in Sec. III. Finally, we provide the summary of the present work in Sec. IV.

II. MODEL

We consider N number of spherical shaped nanoparticles arranged on $l_x \times l_y$ two-dimensional lattice. Let the lattice constant be a and the particle diameter be D , as depicted in Fig. 1(a). Each nanoparticle has a magnetic moment $\mu = M_s V$, M_s being the saturation magnetization and $V = \pi D^3/6$ is the MNP volume. The anisotropy axes of all the MNPs are assumed to have the same orientation with respect to the y -axis of the sample as shown in the schematic Fig. 1(a), α is the orientational angle. The choice of aligned anisotropy axis is considered for two reasons: (1) The assembly with aligned anisotropy axes can be realized experimentally [47–49]. They have distinct magnetic features, which could be useful in various applications. (2) It also provides a unique pathway to distinctly analyze the role of dipolar interaction and anisotropy on the relaxation mechanism.

The following relation gives the energy of a single MNP due to magnetocrystalline anisotropy [46, 50]

$$E_K = K_{\text{eff}} V \sin^2 \theta. \quad (1)$$

Here θ is the angle between the anisotropy axis or the easy axis and the magnetic moment. In the absence of interaction, the functional form of Eq. (1) is a symmetric double-well having two energy minima at $\theta = 0$ and π , respectively. An energy maximum of strength $K_{\text{eff}} V$ at $\theta = \pi/2$ separates these minima, also termed as energy barrier. There is a finite probability for the magnetic moment to flip and reverse its direction in the presence of sufficient temperature. The mean time between two flips is known as the Néel relaxation

time τ_N^o and is given by the Néel-Arrhenius equation [14, 46]

$$\tau_N^o = \tau_o \exp(K_{\text{eff}}V/k_B T). \quad (2)$$

Here $\tau_o = (2\nu_o)^{-1}$, $\nu_o \approx 10^{10} \text{ s}^{-1}$ is the attempt frequency. T is the temperature, and k_B is the Boltzmann constant. Eq. (2) is applicable for a single nanoparticle or very dilute assembly of MNPs.

In an assembly, magnetic nanoparticles primarily interact because of dipolar interaction. The energy associated with such interaction can be evaluated using the following expression [51, 52]

$$E_{\text{dip}} = \frac{\mu_o \mu^2}{4\pi a^3} \sum_{j, j \neq i} \left[\frac{\hat{\mu}_i \cdot \hat{\mu}_j - 3(\hat{\mu}_i \cdot \hat{r}_{ij})(\hat{\mu}_j \cdot \hat{r}_{ij})}{(r_{ij}/a)^3} \right]. \quad (3)$$

Here μ_o is the permeability of free space; $\hat{\mu}_i$ and $\hat{\mu}_j$ are the unit vectors for the magnetic moment of i^{th} and j^{th} nanoparticle, respectively, and the center-to-center separation between them is r_{ij} , \hat{r}_{ij} is the corresponding unit vector.

We can calculate the dipolar field $\mu_o \vec{H}_{\text{dip}}$ corresponding to the dipolar interaction as [52, 53]

$$\mu_o \vec{H}_{\text{dip}} = \frac{\mu \mu_o}{4\pi a^3} \sum_{j, j \neq i} \frac{3(\hat{\mu}_j \cdot \hat{r}_{ij})\hat{r}_{ij} - \hat{\mu}_j}{(r_{ij}/a)^3}. \quad (4)$$

Eq. (3) and Eq. (4) clearly suggest that the strength of this long-ranged interaction varies as $1/r_{ij}^3$. Therefore, we can define a parameter $h_d = D^3/a^3$ [54] to model the dipolar interaction strength. As $h_d = 1.0$ implies $D = a$, the separation between the two nearest neighbouring MNP is the least. Consequently, the dipolar interaction strength is the maximum in this case. Likewise, $h_d = 0$ mimics the non-interacting state. We can write the total energy of the system as [46, 53]

$$E = K_{\text{eff}}V \sum_i \sin^2 \theta_i + \frac{\mu_o \mu^2}{4\pi a^3} \sum_{j, j \neq i} \left[\frac{\hat{\mu}_i \cdot \hat{\mu}_j - 3(\hat{\mu}_i \cdot \hat{r}_{ij})(\hat{\mu}_j \cdot \hat{r}_{ij})}{(r_{ij}/a)^3} \right] \quad (5)$$

It is clearly evident from the above discussion that the single-particle energy function Eq. (1) gets altered because of dipolar interaction. Consequently, the modified energy function has new energy extrema. Let these energy minima be E_1 and E_2 and maxima E_3 . In the presence of thermal fluctuations, the magnetic moment tends to change its orientation. Therefore, the rate ν_1 at which the magnetic moment goes from E_1 to E_2 via E_3 can be

expressed as [55]

$$\nu_1 = \nu_1^0 \exp\left(-\frac{E_3 - E_1}{k_B T}\right) \quad (6)$$

Similarly, the jump rate ν_2 for the magnetic moment to switch its direction from E_2 to E_1 is given by [55]

$$\nu_2 = \nu_2^0 \exp\left(-\frac{E_3 - E_2}{k_B T}\right), \quad (7)$$

Here $\nu_1^0 = \nu_2^0 = \nu_o$.

We have used the kinetic Monte Carlo simulation technique to analyze magnetic relaxation. We have used the same algorithm in the present work, described in detail in the references [36, 46, 53]. Therefore, we do not reiterate it to avoid repetitions. In this procedure, we first saturate all the magnetic moments along the y -direction of the system by applying a huge magnetic field of strength $\mu_o H_o = 20$ T. Next, we divide the total simulation time into 2000 equal steps and switch off the external field $\mu_o H_o$ at $t = 0$ s. We then study the time evolution of magnetization of the underlying system using the kMC simulation. Finally, we fit the so-obtained magnetization-decay curve with $M(t) = M_s \exp(-t/\tau_N)$ to extract effective Néel relaxation time τ_N of the underlying system.

III. SIMULATIONS RESULTS

We consider spherical nanoparticles of magnetite (Fe_3O_4) with the following values of system parameters: $D = 8$ nm, $K_{\text{eff}} = 13 \times 10^3$ Jm⁻³, $M_s = 4.77 \times 10^5$ Am⁻¹, and $T = 300$ K. The total number of MNPs considered as $N = 400$. We have considered six values of system sizes viz. $l_x \times l_y = 20 \times 20, 10 \times 40, 8 \times 50, 4 \times 100, 2 \times 200$ and 1×400 . The corresponding aspect ratio $A_r (= l_y/l_x)$ of the underlying system is 1.0, 4.0, 6.25, 25, 100 and 400, respectively. The dipolar interaction strength h_d is varied from 0 to 1.0. We varied the anisotropy axis orientation angle α between 0 to 90°.

To validate the kMC method implemented in the present work, we first probe the relaxation characteristics without any magnetic interaction. In Fig. 1(b), we plot the simulated magnetization-decay $M(t)/M_s$ versus t curve of a square array of MNPs ($l_x \times l_y = 20 \times 20$, $A_r = 1.0$) with $h_d = 0.0$ and perfectly aligned anisotropy, i.e. $\alpha = 0^\circ$. The functional form of the magnetization decay curve is exponentially decaying. We fit the simulated curve with $M(t)/M_s = \exp(-t/\tau_N^o)$, which yields $\tau_N^o = 1.164 \times 10^{-10} \pm 1.25 \times 10^{-11}$ s. The theoretical value of τ_N^o [using Eq. (2)] comes out to be 1.160×10^{-10} s, which shows perfect agreement

with the simulation and also authenticates the kMC procedure used. In the absence of dipolar interaction, the magnetic relaxation curve is independent of A_r and α . Therefore, the corresponding curves are not shown to avoid duplication.

Next, we study the dipolar interaction and anisotropy axis orientation effect on the magnetic relaxation in a square assembly of MNPs. In Fig. (2), we plot $M(t)/M_s$ versus t curve with $A_r = 1.0$ for six typical values of $\alpha = 0, 30, 45, 60, 75$, and 90° . We have also considered six representative values of $h_d = 0.0, 0.2, 0.4, 0.6, 0.8$, and 1.0 . Irrespective of α , the functional form of the magnetization-decay curve is perfectly exponentially decaying for weak dipolar interaction $h_d \leq 0.3$. There exists a transition point at $h_d \approx 0.4$; magnetization relaxes slowly for $\alpha \leq 45^\circ$. While with $\alpha > 45^\circ$, magnetization decays rapidly. Remarkably, there is a fastening in magnetization relaxation with large dipolar interaction strength ($h_d > 0.4$) compared to weakly interacting MNPs. It can be attributed to enhanced antiferromagnetic coupling because of dipolar interaction in the square arrangement of MNPs. Interestingly, the relaxation characteristics depend very weakly on the orientation of anisotropy axes for a given interaction strength. It could be due to the symmetric nature of the system. Figueiredo *et al.* also observed exponential decay of magnetization for weakly interacting MNPs [56]. The observation of fastening of magnetic relaxation due to antiferromagnetic coupling induced by dipolar interaction is in perfect agreement with our recent work [52]. We found characteristic magnetic hysteresis of antiferromagnetic dominance in a square arrangement of MNPs [52]. De'Bell *et al.* also obtained the minimum energy state to be antiferromagnetic in the square array [57].

The easy axes orientation should affect the relaxation characteristics in an anisotropic system ($A_r \neq 1$). Therefore, we now analyze the time evolution of magnetization with $A_r = 4.0$. In Fig. (3), we plot the magnetization-decay $M(t)/M_s$ vs. t for $A_r = 4.0$ and six values of $\alpha = 0, 30, 45, 60, 75$, and 90° . All other parameters are the same as that of Fig. (2). The magnetization relaxation curve is perfectly exponentially decaying for the small dipolar interaction strength ($h_d \leq 0.2$), similar to that of $A_r = 1.0$. In the presence of moderate dipolar interaction ($h_d \approx 0.4$), the magnetization-decay gets slower for $\alpha \leq 45^\circ$. On the other hand, there is a fastening in the magnetic relaxation with $\alpha > 45^\circ$. In the presence of large dipolar interaction strength, the anisotropy axes orientation affects the relaxation characteristics strongly as anticipated. The magnetization ceases to relax for $\alpha \leq 30^\circ$ with $h_d \approx 0.6$; it relaxes faster for $\alpha > 30^\circ$. The decay of magnetization is extremely rapid for

$h_d > 0.6$, irrespective of α . It is because the strength of antiferromagnetic coupling induced by the dipolar interaction is the maximum in these cases. These results clearly indicate that we can manipulate the nature of the relaxation (slowing or fastening) in a more controlled way by varying h_d and α , which is an essential quantifier in spintronics based applications.

We next study the time evolution of magnetization in the systems with very large aspect ratios. We plot the magnetization-decay $M(t)/M_s$ versus t curves for $A_r = 25.0$ and 100 in Fig. (4) and Fig. (5), respectively. All other parameters are the same as that of Fig. (3). In the absence of dipolar interaction ($h_d = 0.0$), the magnetization relaxation curve is perfectly exponentially decaying, similar to that of the square arrangement of MNPs ($A_r = 1.0$). The direction of anisotropy axes starts to affect the relaxation properties even with weakly interacting MNPs ($h_d \approx 0.2$). In this case, there is a fastening of magnetic relaxation as α is varied from 0 to 90° . In the presence of moderate dipolar interaction ($h_d \approx 0.4$), the magnetization relaxes slowly for $\alpha \leq 45^\circ$. There is a fastening in the magnetic relaxation with $\alpha > 45^\circ$. In the case of enormous dipolar interaction strength ($h_d \geq 0.6$), the magnetization does not relax at all for perfectly aligned anisotropy ($\alpha = 0^\circ$); the same is true for $\alpha \leq 60^\circ$. The magnetization decays extremely rapidly for $\alpha > 60^\circ$ and large dipolar interaction strength $h_d > 0.6$.

To understand the effect of anisotropy axis orientation on magnetic relaxation in a system with a huge aspect ratio, we study the time evolution of magnetization for $A_r = 400$ in Fig. (6); the system corresponds to a one-dimensional array of MNPs. All other parameters are the same as that of Fig. (5). The functional form of the magnetization is exponentially decaying for non-interacting MNPs array ($h_d = 0.0$), irrespective of α as expected. There is a strong effect of α on the rate of magnetization-decay even with weakly interacting MNPs ($h_d \approx 0.2$). There is a fastening of magnetization relaxation as α is varied from 0° to 90° for $h_d \approx 0.2$. Interestingly, the magnetization does not relax even with moderate dipolar interaction strength for perfectly aligned anisotropy axes ($\alpha = 0^\circ$). It is because the dipolar interaction promotes ferromagnetic coupling in this case [46]. There is a rapid decay of magnetization as α is varied from 0 to 90° . Remarkably, all the magnetic moments of the system change their directions from the saturated state (along y -direction) $+1$ to -1 (along $-y$ -direction) in unison, resulting in a complete reversal of magnetization [$M(t)/M_s = -1$] for $\alpha > 60^\circ$. It is due to the fact that the dipolar field and anisotropy axis are antiparallel to each other in such cases [46]. As a consequence, magnetic moment momentarily reverses

their orientations as soon as the external field is removed. The fastening and slowing down of magnetic relaxation with α and h_d is in qualitative agreement with the work of Laslett *et al.* and Hovorka *et al.* [58, 59].

Finally, we study the variation of τ_N as a function of h_d and α in Fig. (7). We have varied α between 0 to 90° and h_d from 0 to 1.0. We have considered six representative values of aspect ratio A_r of the system. In the presence of weak dipolar interaction ($h_d < 0.4$), τ_N does not depend on the direction of the anisotropy axes, i.e. α with $A_r \leq 25.0$. While for large dipolar interaction strength, τ_N decreases with α . τ_N depends strongly on α in the highly anisotropic system even with moderate dipolar interaction strength. In the case of perfectly aligned anisotropy axes, τ_N is the maximum. It is because the strength of ferromagnetic coupling is largest in such a case. There is a rapid decrease in τ_N as α is incremented from 0 to 90°. It is due to the fact that the dipolar field tends to get aligned antiparallel to the direction of the anisotropy axis as α is varied from 0 to 90°. Consequently, magnetization reverses its direction very rapidly as soon as the external magnetic field is switched off. These results can be used in choosing precise values of aspect ratio, dipolar interaction strength and anisotropy axis orientational angle to obtain the desired relaxation time, which could be useful in digital information storages applications.

IV. SUMMARY AND CONCLUSION

Now we summarize the main results presented in this work. In the presence of negligible and small dipolar interaction strength ($h_d \leq 0.2$), the functional form of the magnetization-decay curve is perfectly exponentially decaying. The effective Néel relaxation time τ_N evaluated extracted from the simulated relaxation curve is also in perfect agreement with the value obtained using analytical calculation [using Eq. (2)]. The magnetization relaxation characteristics are found to be independent of anisotropy axes orientation angle α in the system with aspect ratio $A_r \leq 6$. In these cases, a transition point is observed at $h_d = 0.4$; time magnetization-decay dynamics gets slower for $\alpha \leq 45^\circ$. On the other hand, magnetization relaxes rapidly with $\alpha > 45^\circ$. Irrespective of α , magnetization decays very rapidly for large dipolar interaction strength $h_d > 0.6$. This fastening of magnetization relaxation is due to enhanced antiferromagnetic coupling induced by dipolar interaction. In the case of large dipolar interaction strength, MacIsaac *et al.* also observed the dominance of anti-

ferromagnetic coupling in the square array of magnetic moments in the case of large dipolar interaction strength [24]. Our observations are also in perfect qualitative agreement with the work of De’Bell *et al.* [57].

In a highly anisotropic system, the anisotropy axes orientation strongly affects the magnetic relaxation mechanism even in the presence of small dipolar interaction ($h_d \approx 0.2$). We observe fastening of magnetization relaxation as α is incremented from the perfectly aligned case ($\alpha = 0^\circ$) to the perpendicular situation ($\alpha = 90^\circ$). On the other hand, magnetization does not relax at all with $\alpha \leq 60^\circ$ for strongly dipolar interacting MNPs ($h_d > 0.6$). The magnetization decays rapidly for $\alpha > 60^\circ$. Interesting physics emerges in the case of huge $A_r = 400$. Even in the case of weakly dipolar interacting MNPs, there is a rapid decay of magnetization with α . Remarkably, magnetization ceases to relax even with moderate dipolar interaction ($h_d = 0.4$) and perfectly aligned anisotropy ($\alpha = 0^\circ$). It is because dipolar interaction promotes ferromagnetic coupling in such a case. Magnetization decays extremely rapidly as α is varied from 0 to 90° . Interestingly, there is a complete magnetization reversal from saturation (+1) to -1 state with $\alpha > 60^\circ$. In these cases, the anisotropy axes and dipolar field are antiparallel to each other [46]. Consequently, magnetic moments find it easier to reverse their orientations as soon as the external magnetic field is switched off. The effective Néel relaxation time τ_N is also found to significantly affected by dipolar interaction strength, anisotropy axes orientation and aspect ratio of the system. τ_N depends weakly on α for small dipolar interaction and $A_r \leq 25.0$. On the other hand, it decreases rapidly with α for appreciable h_d . In the case of the system with a very high aspect ratio, τ_N depends strongly on α even with moderate values of h_d . In such a case, there is a rapid fall in τ_N as α is incremented from 0 to 90° . It is clearly evident that the presence of antiferromagnetic or ferromagnetic interactions depends strongly on the the angle between the chain axis and the easy axis of the particle, i.e. α in the case of highly anisotropic system (huge A_r). The latter plays an crucial role in fastening or a slowing down of the relaxation.

In conclusion, we have analyzed the effect of dipolar interaction, aspect ratio and anisotropy axes orientation on the magnetic relaxation characteristics in the two-dimensional array of magnetic nanoparticles using kinetic Monte Carlo simulation. The assumption of common anisotropy axes provides extra control in manipulating the relaxation properties computationally. Our consideration of aligned anisotropy also provides the freedom to study the change in the nature of dipolar interactions from ferromagnetic to antiferromagnetic by

manoeuvring the strength of dipolar interaction and orientation of the easy axis. There is a strong effect of these parameters on the magnetization relaxation. Furthermore, the magnetic relaxation characteristics depend strongly on the anisotropy axes orientation for weakly interacting MNPs. Our results are beneficial for applications in data storage and energy storages where such controlled magnetization alignment and desired structural anisotropy is desirable. The observation made in the present article should also help the experimentalists to manipulate the relaxation characteristics of dipolar interacting self-assembled arrays of MNPs in a more controlled manner.

-
- [1] N. Leo, S. Hostenstein, D. Schildknecht, O. Sendetskyi, H. Luetkens, P. M. Derlet, V. Scagnoli, D. Lançon, J. R. Mardegan, T. Prokscha, *et al.*, *Nature Communications* **9**, 1 (2018).
 - [2] V. F. Puentes, P. Gorostiza, D. M. Aruguete, N. G. Bastus, and A. P. Alivisatos, *Nature Materials* **3**, 263 (2004).
 - [3] Z. Mohammadpour and K. Majidzadeh-A, *ACS Biomaterials Science & Engineering* **6**, 1852 (2020).
 - [4] A. Farhan, P. Derlet, A. Kleibert, A. Balan, R. Chopdekar, M. Wyss, L. Anghinolfi, F. Nolting, and L. J. Heyderman, *Nature Physics* **9**, 375 (2013).
 - [5] D. Kechrakos and K. Trohidou, *Applied Physics Letters* **81**, 4574 (2002).
 - [6] T. Wang, Y. Wang, Y. Fu, T. Hasegawa, T. Washiya, H. Saito, S. Ishio, F. Li, H. Oshima, K. Itoh, *et al.*, *Applied Physics Letters* **92**, 192504 (2008).
 - [7] A. Bupathy, V. Banerjee, and J. Carrey, *Physical Review B* **100**, 064420 (2019).
 - [8] S. Ota and Y. Takemura, *The Journal of Physical Chemistry C* **123**, 28859 (2019).
 - [9] X. Waintal and P. W. Brouwer, *Physical review letters* **91**, 247201 (2003).
 - [10] F. Fabris, E. Lima, E. De Biasi, H. E. Troiani, M. V. Mansilla, T. E. Torres, R. F. Pacheco, M. R. Ibarra, G. F. Goya, R. D. Zysler, *et al.*, *Nanoscale* **11**, 3164 (2019).
 - [11] R. Hergt, S. Dutz, and M. Zeisberger, *Nanotechnology* **21**, 015706 (2009).
 - [12] R. J. Tackett, J. Thakur, N. Mosher, E. Perkins-Harbin, R. E. Kumon, L. Wang, C. Rablau, and P. P. Vaishnav, *Journal of Applied Physics* **118**, 064701 (2015).
 - [13] W. Wernsdorfer, E. B. Orozco, K. Hasselbach, A. Benoit, B. Barbara, N. Demoncy, A. Loiseau, H. Pascard, and D. Mailly, *Physical Review Letters* **78**, 1791 (1997).

- [14] J. Carrey, B. Mehdaoui, and M. Respaud, *Journal of Applied Physics* **109**, 083921 (2011).
- [15] M. Anand, J. Carrey, and V. Banerjee, *Physical Review B* **94**, 094425 (2016).
- [16] M. Anand, J. Carrey, and V. Banerjee, *Journal of Magnetism and Magnetic Materials* **454**, 23 (2018).
- [17] K. Konwar, S. D. Kaushik, D. Sen, and P. Deb, *Physical Review B* **102**, 174449 (2020).
- [18] D. Parker, V. Dupuis, F. Ladieu, J.-P. Bouchaud, E. Dubois, R. Perzynski, and E. Vincent, *Physical Review B* **77**, 104428 (2008).
- [19] P. J. Santos and R. J. Macfarlane, *Journal of the American Chemical Society* **142**, 1170 (2020).
- [20] S. Mørup, M. F. Hansen, and C. Frandsen, *Beilstein journal of nanotechnology* **1**, 182 (2010).
- [21] M. Holden, M. Plumer, I. Saika-Voivod, and B. Southern, *Physical Review B* **91**, 224425 (2015).
- [22] A. Bailly-Reyre and H. T. Diep, *Journal of Magnetism and Magnetic Materials* **528**, 167813 (2021).
- [23] J. Luttinger and L. Tisza, *Physical Review* **70**, 954 (1946).
- [24] A. MacIsaac, J. Whitehead, K. De'Bell, and P. Poole, *Physical review letters* **77**, 739 (1996).
- [25] P. Politi, M. G. Pini, and R. Stamps, *Physical Review B* **73**, 020405 (2006).
- [26] P.-M. Déjardin, *Journal of Applied Physics* **110**, 113921 (2011).
- [27] Ò. Iglesias and A. Labarta, *Physical Review B* **70**, 144401 (2004).
- [28] S.-H. Liao, H.-S. Huang, J.-H. Chen, Y.-K. Su, and Y.-F. Tong, *RSC Advances* **8**, 4057 (2018).
- [29] M. Anand, *Journal of Magnetism and Magnetic Materials* **522**, 167538 (2021).
- [30] D. Gallina and G. Pastor, *Physical Review X* **10**, 021068 (2020).
- [31] P. Ilg, *Physical Review B* **95**, 214427 (2017).
- [32] S. Denisov and K. Trohidou, *physica status solidi (a)* **189**, 265 (2002).
- [33] S. Shtrikman and E. Wohlfarth, *Physics Letters A* **85**, 467 (1981).
- [34] J. Dormann, L. Bessais, and D. Fiorani, *Journal of Physics C: Solid State Physics* **21**, 2015 (1988).
- [35] S. Mørup and E. Tronc, *Physical Review Letters* **72**, 3278 (1994).
- [36] M. Anand, arXiv preprint arXiv:2105.00472 (2021).
- [37] D. P. Valdés, E. Lima Jr, R. D. Zysler, and E. De Biasi, *Physical Review Applied* **14**, 014023 (2020).

- [38] C. Jiang, C. W. Leung, and P. W. Pong, *Nanoscale research letters* **11**, 1 (2016).
- [39] M. Anand, *Journal of Applied Physics* **128**, 023903 (2020).
- [40] C. Martinez-Boubeta, K. Simeonidis, A. Makridis, M. Angelakeris, O. Iglesias, P. Guardia, A. Cabot, L. Yedra, S. Estradé, F. Peiró, *et al.*, *Scientific reports* **3**, 1 (2013).
- [41] D. Serantes, K. Simeonidis, M. Angelakeris, O. Chubykalo-Fesenko, M. Marciello, M. D. P. Morales, D. Baldomir, and C. Martinez-Boubeta, *The Journal of Physical Chemistry C* **118**, 5927 (2014).
- [42] I. Conde-Leborán, D. Serantes, and D. Baldomir, *Journal of Magnetism and Magnetic Materials* **380**, 321 (2015).
- [43] Z. Boekelheide, J. T. Miller, C. Grüttner, and C. L. Dennis, *Journal of applied physics* **126**, 043903 (2019).
- [44] Q. Li, C. W. Kartikowati, T. Iwaki, K. Okuyama, and T. Ogi, *Royal Society Open Science* **7**, 191656 (2020).
- [45] P. Allia, G. Barrera, and P. Tiberto, *Journal of Magnetism and Magnetic Materials* **496**, 165927 (2020).
- [46] M. Anand, V. Banerjee, and J. Carrey, *Physical Review B* **99**, 024402 (2019).
- [47] K. Deng, Z. Luo, L. Tan, and Z. Quan, *Chemical Society Reviews* **49**, 6002 (2020).
- [48] T. Wen, Y. Li, D. Zhang, Q. Zhan, Q. Wen, Y. Liao, Y. Xie, H. Zhang, C. Liu, L. Jin, *et al.*, *Journal of colloid and interface science* **497**, 14 (2017).
- [49] C. Jiang, D. Oshima, S. Iwata, P. W. Pong, and T. Kato, *Journal of Nanoparticle Research* **22**, 1 (2020).
- [50] G. Muscas, G. Concas, S. Laureti, A. Testa, R. Mathieu, J. De Toro, C. Cannas, A. Musinu, M. Novak, C. Sangregorio, *et al.*, *Physical Chemistry Chemical Physics* **20**, 28634 (2018).
- [51] N. Usov, O. Serebryakova, and V. Tarasov, *Nanoscale Research Letters* **12**, 1 (2017).
- [52] M. Anand, arXiv preprint arXiv:2104.02961 (2021).
- [53] R. Tan, J. Carrey, and M. Respaud, *Physical Review B* **90**, 214421 (2014).
- [54] R. Tan, J. Lee, J. Cho, S. Noh, D. Kim, and Y. Kim, *Journal of Physics D: Applied Physics* **43**, 165002 (2010).
- [55] P. Hänggi, P. Talkner, and M. Borkovec, *Reviews of Modern Physics* **62**, 251 (1990).
- [56] W. Figueiredo and W. Schwarzacher, *Journal of Physics: Condensed Matter* **19**, 276203 (2007).

- [57] K. De'Bell, A. MacIsaac, I. Booth, and J. Whitehead, *Physical Review B* **55**, 15108 (1997).
- [58] O. Laslett, S. Ruta, R. Chantrell, J. Barker, G. Friedman, and O. Hovorka, *Physica B: Condensed Matter* **486**, 173 (2016).
- [59] O. Hovorka, J. Barker, G. Friedman, and R. Chantrell, *Physical Review B* **89**, 104410 (2014).

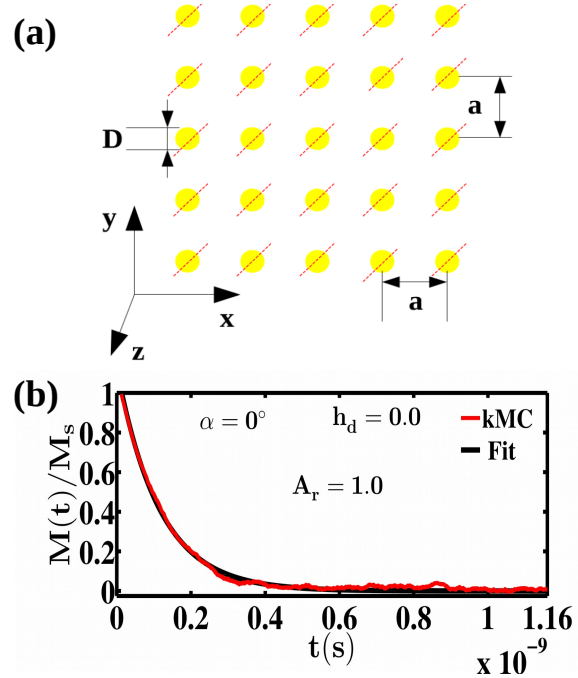


FIG. 1: (a) Schematic of the two-dimensional array of magnetic nanoparticles. The diameter of the nanoparticle is D , and a is the lattice spacing. The dashed line denotes the direction of the anisotropy axis. All the particles are assumed to have the same anisotropy axes orientations, α being the angle with respect to the y -axis. (b) Magnetization-decay $M(t)/M_s$ vs. t curve for non-interacting MNPs ($h_d = 0.0$) with $A_r = 1.0$ and perfectly aligned anisotropy axes ($\alpha = 0^\circ$). We have fitted the simulated curve with $M(t)/M_s = \exp(-t/\tau_N^o)$ and shown it with a black line. In the absence of magnetic interaction, the form of the relaxation curve does not depend on A_r and α (curves not shown).

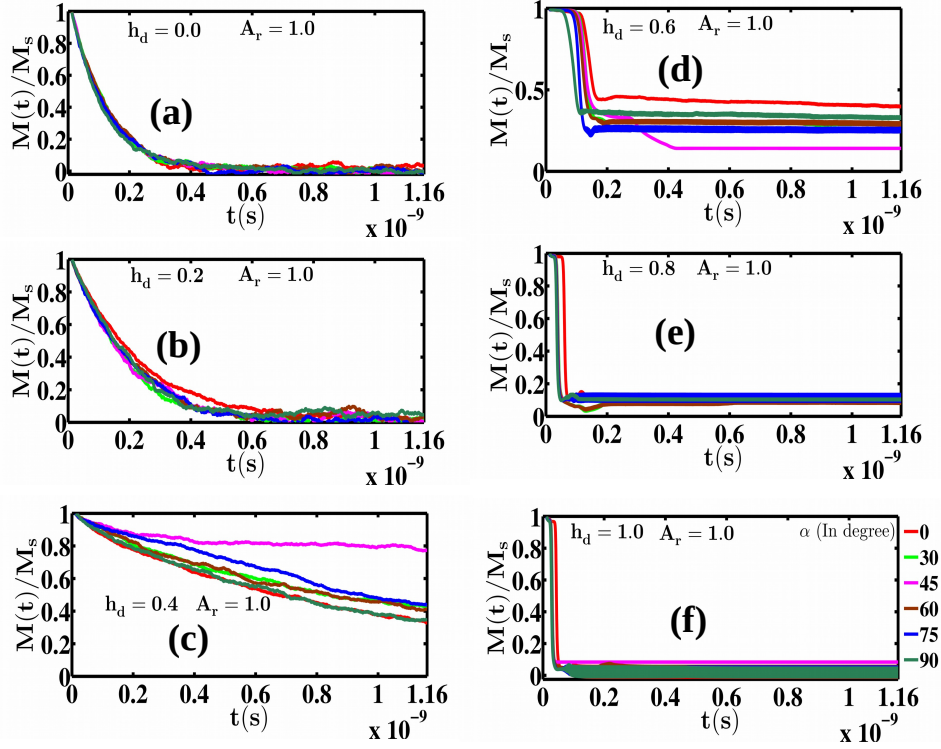


FIG. 2: Magnetization-decay $M(t)/M_s$ versus t curves as a function of anisotropy axes orientation angle α with the square arrangement of MNPs ($A_r = 1.0$). We have considered six representative values of h_d : (a) $h_d = 0.0$, (b) $h_d = 0.2$, (c) $h_d = 0.4$, (d) $h_d = 0.6$, (e) $h_d = 0.8$, and (f) $h_d = 1.0$. In the presence of small $h_d \leq 0.3$, the magnetization-decay curve is perfectly exponentially decaying. Interestingly, magnetization decays faster for large h_d in comparison with weakly interacting MNPs. There is also a weak dependence of the relaxation characteristics on α for a fixed h_d .

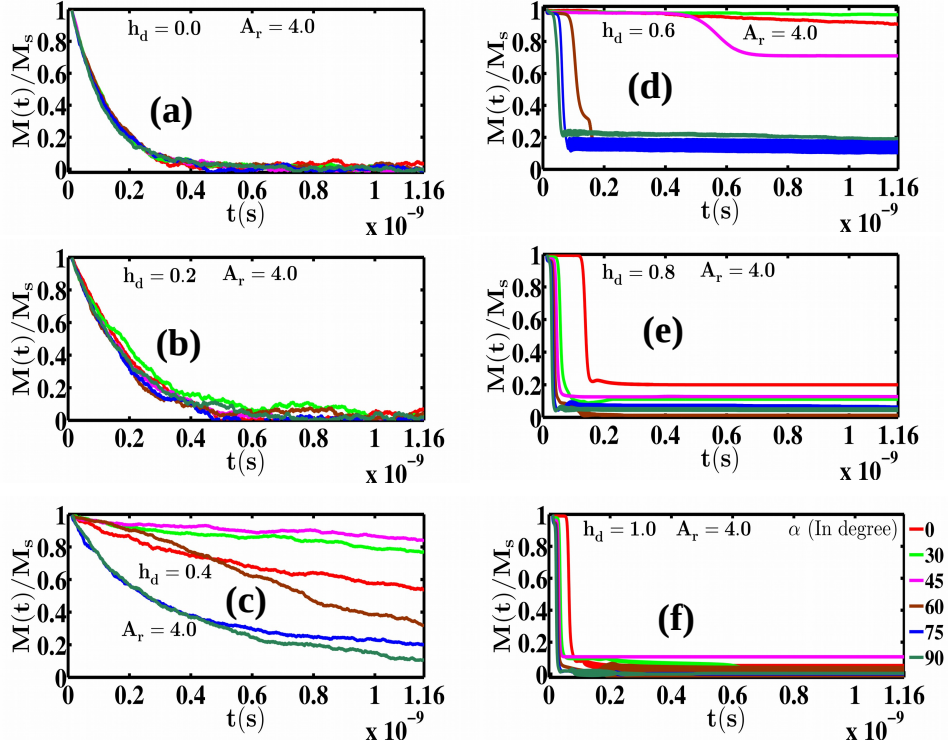


FIG. 3: Time evolution of magnetization as a function of α for various values of h_d with $A_r = 4.0$. We have considered six representative values of h_d : (a) $h_d = 0.0$, (b) $h_d = 0.2$, (c) $h_d = 0.4$, (d) $h_d = 0.6$, (e) $h_d = 0.8$, and (f) $h_d = 1.0$. The magnetization decays slowly for $\alpha \leq 45^\circ$ with moderate dipolar interaction strength h_d . On the other hand, there is rapid decay of magnetization with $\alpha > 45^\circ$. Irrespective of α , magnetization decays rapidly for large h_d as compared to weakly dipolar interacting case.

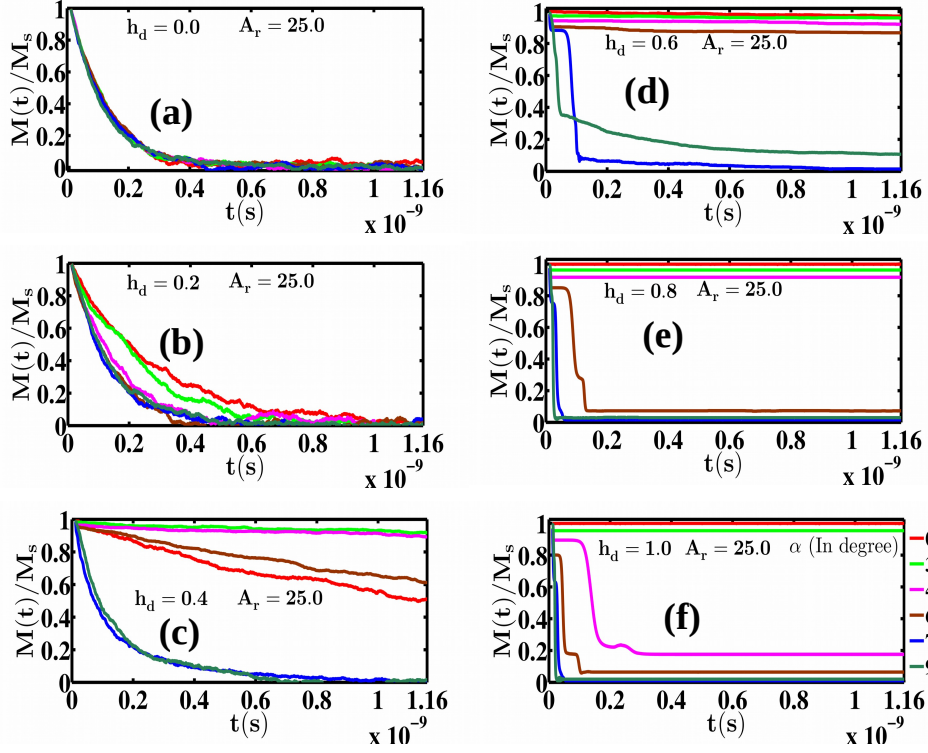


FIG. 4: Magnetization-decay curves as a function of anisotropy axes orientation with $A_r = 25.0$. We have considered six representative values of h_d : (a) $h_d = 0.0$, (b) $h_d = 0.2$, (c) $h_d = 0.4$, (d) $h_d = 0.6$, (e) $h_d = 0.8$, and (f) $h_d = 1.0$. Relaxation characteristics is greatly affected by α even for small h_d . Magnetization decays very rapidly as α is varied from 0 to 90°. Remarkably, magnetization ceases to relax with perfectly aligned anisotropy ($\alpha = 0^\circ$) and large h_d because of enhancement in ferromagnetic coupling. There is also a fastening in magnetic relaxation for $\alpha > 60^\circ$.

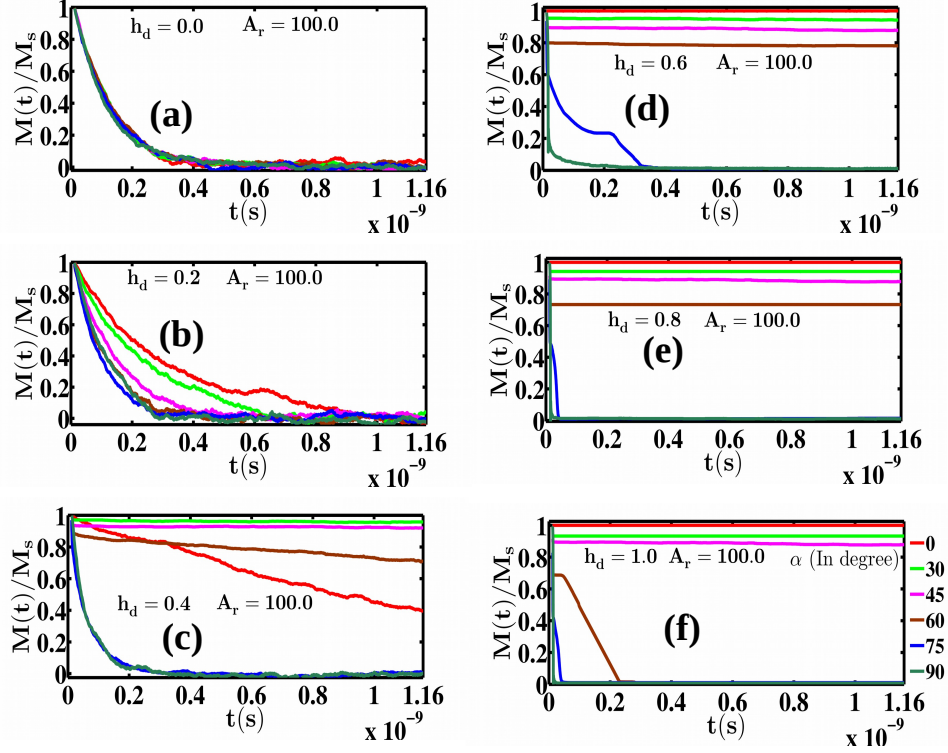


FIG. 5: Magnetization relaxation curves for various of h_d and α with very large aspect ratio $A_r = 100$. We have considered six representative values of h_d : (a) $h_d = 0.0$, (b) $h_d = 0.2$, (c) $h_d = 0.4$, (d) $h_d = 0.6$, (e) $h_d = 0.8$, and (f) $h_d = 1.0$. There is a fastening in magnetization-decay with α even in the case of weakly interacting MNPs. While for large h_d , magnetization relaxes extremely slowly for $\alpha \leq 45^\circ$. Interestingly, the magnetization decays extremely rapidly for $\alpha > 60^\circ$ in such a case.

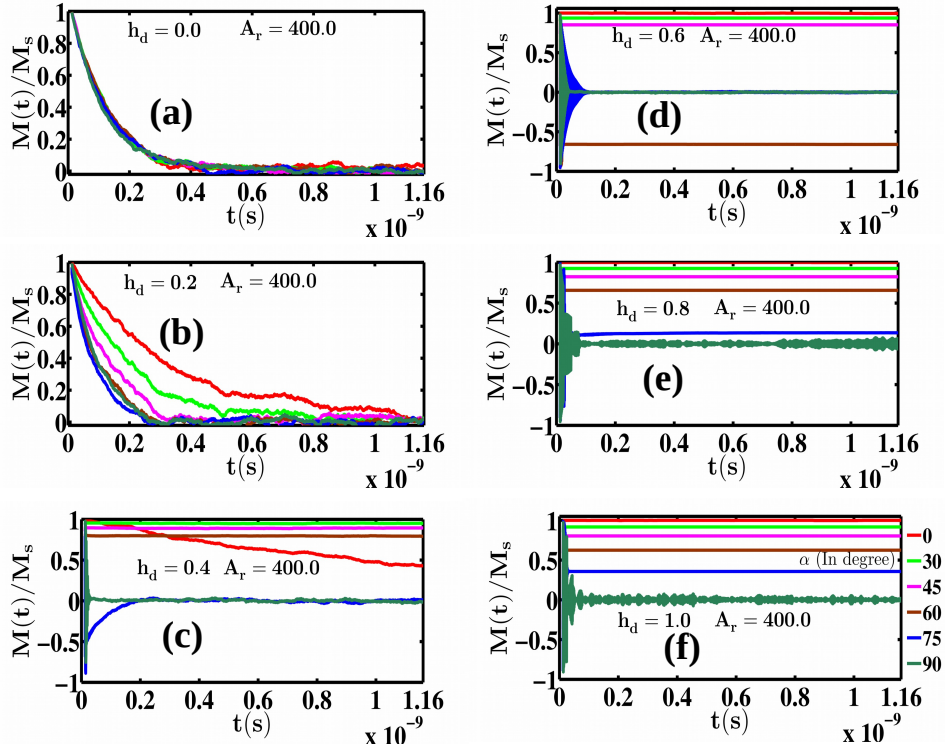


FIG. 6: Magnetization-decay $M(t)/M_s$ versus t curves for huge $A_r = 400$ as a function of α and h_d . We have considered six representative values of h_d : (a) $h_d = 0.0$, (b) $h_d = 0.2$, (c) $h_d = 0.4$, (d) $h_d = 0.6$, (e) $h_d = 0.8$, and (f) $h_d = 1.0$. There is a strong effect of α on the rate of magnetization-decay even with a small $h_d = 0.2$. There is a rapid decay of magnetization with α in this case. Interestingly, the magnetization does not relax even with moderate values of h_d and $\alpha = 0^\circ$. In the presence of moderate dipolar interaction and $\alpha > 60^\circ$, there is a complete reversal of magnetization from the saturated situation (+1) to -1 state as soon as the external field is removed. The anisotropy axis and dipolar field get aligned antiparallel to each other, which helps the magnetization switch its direction just after removing the external magnetic field.

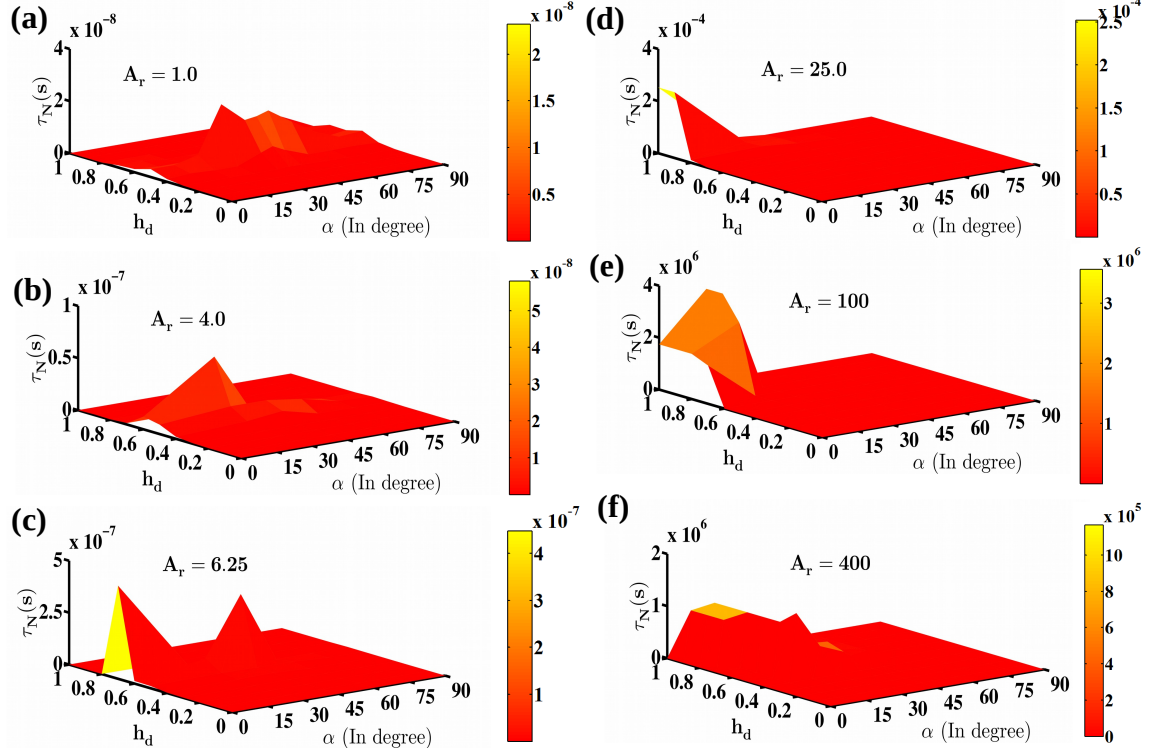


FIG. 7: Variation of effective Neel relaxation time τ_N as a function of h_d and α for various values of A_r . We have considered six representative values of A_r : (a) $A_r = 1.0$, (b) $A_r = 4.0$, (c) $A_r = 6.25$, (d) $A_r = 25.0$, (e) $A_r = 100$, and (f) $A_r = 400$. There is a weak dependence of τ_N on α for small h_d and $A_r \leq 25.0$. While for large h_d , τ_N decreases with α . τ_N depends strongly on α for huge A_r . There is a rapid decrease in τ_N as α is incremented from 0 to 90° .